# Skeletal muscle metastases on magnetic resonance imaging: analysis of 31 cases

**Qi Li[1,2], Lei Wang[2], Shinong Pan[1], Hong Shu[3], Ying Ma[3], Zaiming Lu[1], Xihu Fu[1], Bo Jiang[2], Qiyong Guo[1]**

[1]Department of Radiology, Shengjing Hospital of China Medical University, China
[2]Department of Radiology, Liaoning Electric Power Central Hospital, China
[3]Department of Pathology, Shengjing Hospital of China Medical University, China

**Aim of the study:** To investigate the magnetic resonance imaging (MRI) features of skeletal muscle metastases (SMM).

**Material and methods:** The records of 31 patients with proven SMM were retrospectively reviewed. Clinical history, type of primary malignancy, location of metastases, and MRI features of SMM were evaluated. Based on MRI findings, SMM were divided into three MRI types. The correlation between MRI types with ages and pathology category, between MRI types of SMM and ages, as well as MRI types of SMM and pathology category were analysed with Spearman's rho.

**Results:** The most common primary tumour was genital tumour (25.8%) and bronchial carcinoma (19.4%), and the most common cell type was adenocarcinoma (58.1%). SMM were located in the iliopsoas muscle (26.3%), paravertebral muscles (21.1%), and upper extremity muscles (18.4%). MRI features: (1) Type-I localised lesions (12.90%), round-like mass limited to local regions with heterogeneous iso-signal intensity in T1WI and heterogeneous hyper-intensity in T2WI; (2) Type-II diffuse lesions without bone destruction (35.48%), abnormal diffuse swelling of the muscle with irregular boundaries and slightly hypo- to iso-intensity in T1WI and hyper-intensity in T2WI; and (3) Type-III diffuse lesions with bone destruction (51.61%), distinct irregular lump with iso-intensity in T1WI and heterogeneous hyper-intensity in T2WI with adjacent bone invasion. There was positive correlation between MRI types and ages ($r = 0.431$, $p < 0.05$). There were no significant differences of MRI types with pathology category ($p > 0.05$).

**Conclusions:** SMM features on MRI can be broadly used to classify lesions, which is beneficial for SMM diagnosis.

**Key words:** metastases, tumour, skeletal muscle, MRI.

**Contemp Oncol (Pozn) 2016; 20 (3): 242–250**
**DOI: 10.5114/wo.2016.61568**

## Introduction

Skeletal muscle metastases (SMM) are a rare form of malignancy that occur in less than 1% of all metastases [1–3]. However, this number increases greatly at autopsy, where the prevalence of SMM has been reported to be between 16 and 17.5% [4, 5]. The discovery of SMM as the initial presenting feature of a potential primary malignant tumour is difficult to ascertain by clinical symptoms and/or imaging findings as it is easily misdiagnosed as a primary soft tissue sarcoma or soft tissue trauma. Because the treatment and prognosis of SMM are highly specific, it is extremely important to achieve an accurate diagnosis.

Surov *et al*. [4] compiled data for SMM with respect to the site of the primary tumour, prevalence, and computed tomography (CT) findings. As is well known, magnetic resonance imaging (MRI) offers higher resolution imaging of soft tissue than CT and provides greater accuracy in the diagnosis of soft tissue lesions because it is more capable of precisely defining the region of diseased tissue, which allows for a more reliable estimation of disease staging [6, 7]. Increased attention has been paid to the use of MRI for the diagnosis and differential diagnosis of SMM [8–18]; however, there is still no MRI-based classification that could provide additional clinical evidence for disease staging.

Therefore, the present study used MRI information to detect changes of features in SMM. In addition, this paper also discusses the potential value of MRI in the diagnosis of SMM and evaluates the correlation between the features in SMM using MRI and histological changes.

## Material and methods

### Patients

We conducted the imaging data within our institute from January 2005 to December 2013. Inclusion criteria: muscle metastases confirmed through pathology or fine needle aspiration biopsy. Exclusion criteria: (1) history of skeletal muscle trauma; (2) systemic connective tissue disease; (3) surgical history; (4) skeletal muscle primary tumour; and (5) any cases with intramuscular deposits of lymphoma, leukaemia, or primary soft tissue tumour. The study was approved by Shengjing Hospital of China Medical University Medical Ethics Committee. All patients were informed of the purpose of the study, and the individual and (or) their families gave written informed consent for the study and its publication. The patient group consisted of 14 male and 17 female patients aged between 26 and 82 years (mean 57 years). Twenty-four patients complained of pain, 13 patients had localised swelling, and 10 patients had symptoms of both pain and swelling. In 27 patients, the diagnosis of SMM was confirmed by biopsy and in four patients through

pathological examination of the surgical specimen. Among the patients included in the study, 13 had a known primary malignant tumour, and the mean duration from primary malignant tumour diagnosis to SMM was 27 months (range 1–72 months). In 11 cases the SMM was detected first, and in seven cases the primary lesions and metastases were found at the same time.

The skeletal muscle metastases were derived from the following malignancies: genital tumours (25.8%), bronchial carcinoma (19.4%), and urological tumours (16.1%). Other neoplasias were rare. In detail: carcinoma of bronchus (19.4%), carcinoma of cervix uteri (9.7%), carcinoma of ovary (9.7%), renal cell carcinoma (9.7%), endometrial carcinoma (6.5%), hepatocellular carcinoma (6.5%), retroperitoneal tumour (6.5%), carcinoma of prostate (6.5%), carcinoma of unknown primary (6.5%), nasopharyngeal carcinoma (6.5%), carcinoma of colon and rectum (6.5%), carcinoma of thyroid gland (3.2%), and carcinoma of stomach (3.2%). The number and proportion of primary malignancies metastasised into skeletal muscles are given in Table 1. The histological types were as follows: adenocarcinoma ($n$ = 18, 58.1%), squamous cell carcinoma ($n$ = 8, 25.8%), transitional cell carcinoma ($n$ = 2, 6.5%), and malignant fibrous histiocytoma ($n$ = 2, 6.5%); one case ($n$ = 1, 3.2%) had a mesenchyme.

**Table 1.** Primary malignancies metastasised into skeletal muscles

| Primary tumours | The number and proportion of SMM (%) |
|---|---|
| Carcinoma of bronchus | 6 (19.4%) |
| Carcinoma of cervix uteri | 3 (9.7%) |
| Carcinoma of ovary | 3 (9.7%) |
| Renal cell carcinoma | 3 (9.7%) |
| Endometrial carcinoma | 2 (6.5%) |
| Hepatocellular carcinoma | 2 (6.5%) |
| Retroperitoneal tumour | 2 (6.5%) |
| Carcinoma of prostate | 2 (6.5%) |
| Carcinoma of unknown primary | 2 (6.5%) |
| Nasopharyngeal carcinoma | 2 (6.5%) |
| Carcinoma of colon and rectum | 2 (6.5%) |
| Carcinoma of thyroid gland | 1 (3.2%) |
| Carcinoma of stomach | 1 (3.2%) |

### Magnetic resonance imaging

Magnetic resonance imaging was performed with a 3.0 T (Philips Achieve, Best, Netherlands) system. Before surgery, all patients underwent MRI examination. MRI included routine SE T1WI TR/TE = 540/6.88 ms, T2WI TR/TE = 6140/108.11 ms, TSE-SPAIR T2WI: TR/TE = 5100/86.13 ms, matrix = 512 × 512, field of view = 240–420 mm, number of acquisitions = 3. Twenty-six patients also underwent contrast-enhanced MRI with intravenous administration of gadodiamide (Omniscan; GE Healthcare, Piscataway, NJ), 0.2 ml/kg body weight equal to 0.1 mmol/kg, a total of 8.0–15.0 ml, administration time 20–40 seconds.

### Imaging analysis

Clinical records were reviewed with respect to age, gender, site, location, and type of primary tumour. Two radiologists blinded to the experimental design analysed the images. The final results had to be accepted by both radiologists in order for the case to be included in subsequent analyses. A third radiologist was consulted if there was a divergence in the opinion of the two primary radiologists. In the present study, the MRI signal characteristics for SMM were divided into several types according to the following factors: focus morphology, focus distribution, relationship between focus and adjacent tissues, MRI signal distribution characteristics, and destruction of adjacent bone. The MRI characteristics of SMM were statistically analysed.

MRI types were discussed along with the methodology used for CT diagnosis by Surov *et al.* [4]. Based on morphology, location and distribution, the relationship with the lesion and adjacent tissues, signal intensity characteristics on MRI, and destruction of adjacent bone, we divided the MRI types of SMM into a '3 type, 4 subtype system' as follows: Type I: focal lesions, Type II: diffuse lesions without bone destruction, Type III: diffuse lesions with bone destruction, of which Type III-1: small lesion with clear boundary and Type III-2: large lesion with unclear boundary.

### Histopathological analysis

The diagnosis of SMM was confirmed histopathologically in four cases. Needle biopsy was performed in 27 patients. Biopsy specimens were evaluated by two pathologists (S. H. and M. Y. with 25 and 27 years of experience, respectively). In our study, 10 available histological materials (sections stained by haematoxylin/eosin and by immunohistochemistry) were re-analysed. Immunohistochemistry was used to study the expression of CD 4, CD24, CD44, CK, and P63 in these 10 cases.

### Statistical analysis

Statistical analysis was performed with computer software (SPSS, version 16.0 for Windows; Chicago, IL). The number and frequency of each MRI type observed was calculated. The Spearman Rank correlation was used to analyse the correlation between SMM type on MRI and age. $P < 0.01$ was considered statistically significant. In addition, the Spearman Rank correlation was used to evaluate the correlation between SMM type on MRI and pathological category.

## Results

### Localization of skeletal muscle metastases

Of the 31 patients, 27 patients had one SMM, two patients had two, one patient had three, and one patient had four SMM. In total there were 38 lesions from 31 patients, metastases were identified in the iliopsoas muscle (26.3%), in the paravertebral muscles (21.1%), and in upper extremity muscles (18.4%). Other locations of SMM were rare. In de-

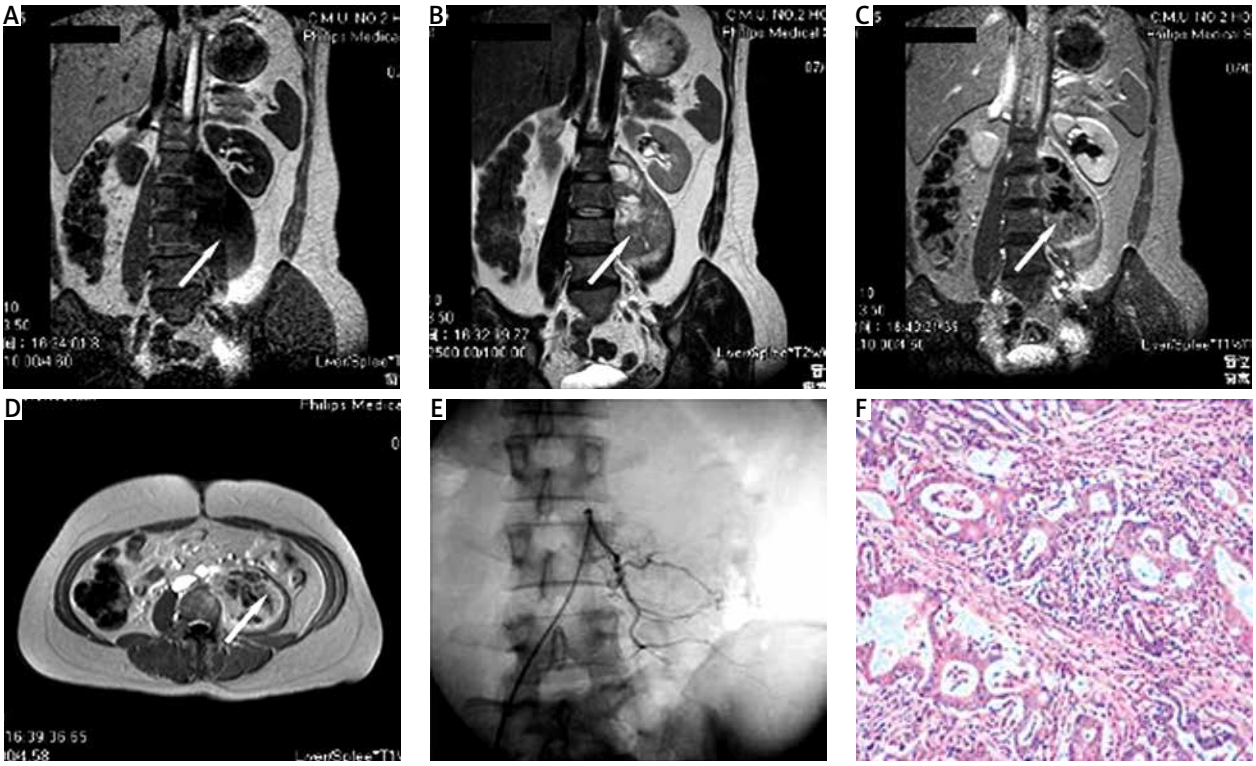


**Fig. 1.** Type I focal lesion in a 41-year-old woman with endometrial carcinoma. The left psoas major was thickened and presented with a round-shaped mass, mainly showing slightly hypointense signal intensity in T1WI and slightly hyperintense signal intensity in T2WI (A, B, arrow). Enhanced MRI showed moderate ring-shaped enhancement with no enhanced irregular areas within the lesion (C, D arrow). DSA shows that the mass presented obvious tumour blush (E). Under the microscope, the cancer cells could be seen to be arranged into adenoid shapes with interstitial fibrosis hyperplasia and more inflammatory cell infiltration (200× magnification). Pathology confirmed that the metastatic lesion was derived from adenocarcinoma (F)

**Table 2.** Location of detected skeletal muscle metastases

| Location of SMM | The number and proportion of SMM (%) |
|---|---|
| Iliopsoas | 10 (26.3%) |
| Psoas major | 5 (13.2%) |
| Quadratus lumborum | 3 (7.9%) |
| Pectoralis | 3 (7.9%) |
| Biceps brachii | 3 (7.9%) |
| Quadriceps femoris | 3 (7.9%) |
| Obliquus abdominis | 2 (5.3%) |
| Gluteus maximus | 2 (5.3%) |
| Biceps femoris | 2 (5.3%) |
| Rectus abdominis | 1 (2.6%) |
| Medial pterygoid | 1 (2.6%) |
| Sternocleidomastoid | 1 (2.6%) |
| Serratus anterior | 1 (2.6%) |
| Adductor longus | 1 (2.6%) |

tail, SMM were identified in the following muscles: iliopsoas ($n$ = 10), quadratus lumborum ($n$ = 3), psoas major ($n$ = 5), rectus abdominis ($n$ = 1), obliquus abdominis ($n$ = 2), medial pterygoid ($n$ = 1), sternocleidomastoid ($n$ = 1), pectoralis ($n$ = 3), biceps brachii ($n$ = 3), serratus anterior ($n$ = 1), gluteus maximus ($n$ = 2), quadriceps femoris ($n$ = 3), biceps femoris ($n$ = 2), and adductor longus ($n$ = 1). SMM involving more than one muscle occurred in four patients.

## Magnetic resonance imaging manifestations of different types of skeletal muscle metastases

The clinical data and MRI manifestations of different types of SMM of the 31 patients are summarised in Table 2. Based on MR findings, SMM was divided into three MR types: (1) Type-I localised lesions (12.90%), round-like mass limited to local regions with heterogeneous iso-signal intensity in T1WI and heterogeneous hyper-intensity in T2WI. Of the Type I-focal lesions (Fig. 1), three cases (75%) showed heterogeneous iso-intensity in T1WI, heterogeneous hyper-intensity in T2WI, coupled with a poorly defined boundary. All of the four cases, three were performed by contrast, and three showed moderate ring-shaped enhancement. (2) Type-II diffuse lesions without bone destruction (35.48%), abnormal diffuse swelling of the muscle with irregular boundaries and slightly hypo- to iso-intensity in T1WI and hyper-intensity in T2WI. Of the Type II-diffuse lesions without bone destruction (Fig. 2), nine cases (81.82%) showed diffuse swelling with irregular and fuzzy boundaries and heterogeneous iso-intensity in T1WI. Ten of the 11 cases (90.91%) showed heterogeneous hyperintensity in both T2WI and TSE-SPAIR T2WI. Of all the 11 cases, 10 cases were performed by contrast, nine cases showed moderate heterogeneous feathery or moderate ring-shaped enhance-

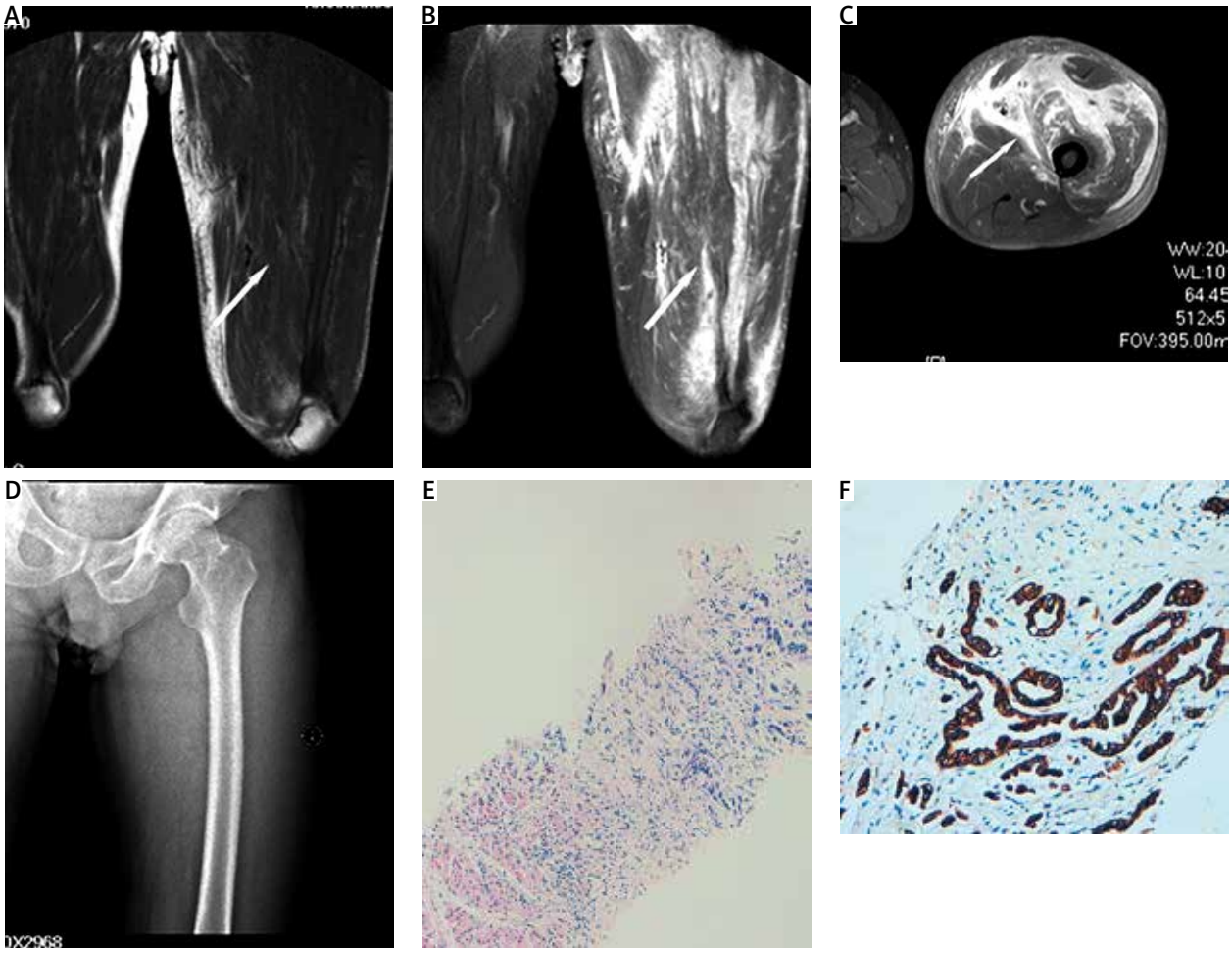


**Fig. 2.** Type II diffuse lesion in a 69-year-old man with stomach carcinoma. The soft tissue around the left quadriceps femoris muscle presented with diffuse swelling, showing iso-signal intensity in T1WI (A, arrow). Enhanced MRI showed irregular and honeycomb-like ring enhancement (B, C, arrow). Radiography showed no signs of bone destruction around the lesion (D). Under the microscope, muscle tissue can be seen at one end of the organisation, and at the other end the cancer cells were arranged in cord-like and irregular tubular shapes with invasive growth (100× magnification). Pathology confirmed adenocarcinoma metastases (E). The immunohistochemical CK staining, cancer tissue showed positive and brown granules as can be seen in the cytoplasm (200× magnification) (F)

ment (9/11), and two cases showed fuzzy and feathery enhancement. (3) Type-III diffuse lesions with bone destruction (51.61%), distinct irregular lump with iso-intensity in T1WI, and heterogeneous hyper-intensity in T2WI with adjacent bone invasion. For the cases with a Type III-diffuse lesion with bone destruction (Figs. 3, 4), MRI showed the presence of an irregular, mixed lump with root-like growth and with adjacent bone invasion presenting as pathological fractures or focal fragments of bone in the irregular lump and/or adjacent region. Eleven of the 16 cases (68.75%) showed diffuse swelling with a fuzzy boundary, and heterogeneous slight iso-intensity in T1WI. All cases showed heterogeneous hyperintensity in T2WI, and 15 of 16 cases (93.75%) also showed heterogeneous hyperintensity in TSE-SPAIR T2WI. For lesions involving soft tissue with or without a clear boundary, the Type III cases were further divided into two subtypes, Type III-1 (Fig. 3) and Type III-2 (Fig. 4). Of all the 16 cases, 13 cases were performed by contrast, 10 cases showed moderate heterogeneous feathery or moderate ring-shaped enhancement (10/16), two cases showed fuzzy enhancement, and one case showed remarkable enhancement.

### Correlation between age and magnetic resonance imaging type of skeletal muscle metastases

The distribution of MRI types of SMM varied between different age groups (Fig. 5). In this study, 28 of 31 patients (90.32%) were more than 40 years old, and 25 of 31 (80.65%) were more than 50 years old. There was a positive correlation between MR type and age ($r$ = 0.431, $p < 0.05$). There were no significant correlations between MR type and pathology category ($p > 0.05$).

### Histological diagnosis

In this study, all biopsy and pathological diagnoses were reviewed by a pathology professor. The typical histological features of the SMM samples showed the disappearance of normal striated muscle structure, the proliferation of fibrous tissue in different proportions, and the arrangement of cancer tissue in adenoid structures, nests, and sheets. Some specimens showed areas of necrosis within the le-

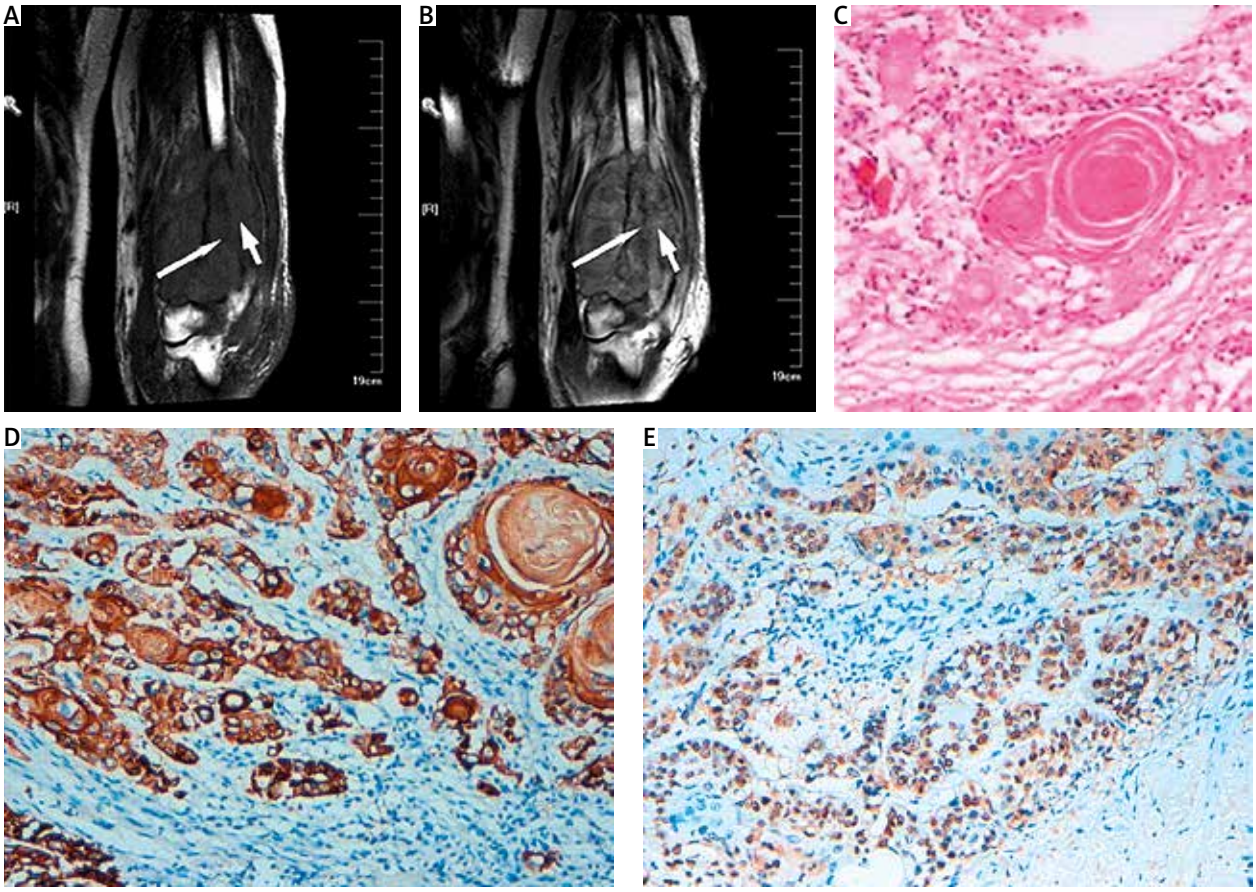


**Fig. 3.** Type III SMM complicated by bone destruction in a 52-year-old man with bronchial carcinoma. The soft tissue of the left biceps brachii presented with swelling and persistent pain. The left distal humorous showed bone destruction and fracture with iso-signal intensity in T1WI (A, arrow) and mixed hypointense iso-signal intensity in T2WI (B, arrow). The surrounding muscles showed irregular iso-signal intensity (A, B, arrowhead). Under the microscope, the cells exhibited enlarged nuclei, anachromasis, and a cancer nest arrangement with a lamellar shape with invasive growth and keratin pearls (200× magnification). Pathology confirmed muscle metastases (C). In the immunohistochemistry CK staining, cancer tissue showed positive and brown granules as can be seen in the cytoplasm (200× magnification) (D). In the immunohistochemistry P63 staining, cancer tissue showed positive and brown granules as can be seen in the cell nucleus (200× magnification) (E)

**Table 3.** TNM stage of the primary tumour in 29 cases

| TNM | Number | Proportion (%) |
|---|---|---|
| IV | 29 | 100 |
| T1 | 6 | 20.7 |
| T2 | 15 | 51.7 |
| T3 | 8 | 27.6 |
| T4 | 0 | 0 |
| N1 | 10 | 34.5 |
| N2 | 8 | 27.6 |
| N3 | 11 | 37.9 |
| M0 | 0 | 0 |
| M1 | 29 | 100 |

sion. In 29 cases with known primary tumours, according to the clinical, radiological, and pathological features of primary disease, we acquired the TNM staging of the primary disease (Table 3) referring to TNM Classification of Malignant Tumors-7th [19]. In the other two cases of unknown primary, one was confirmed as adenocarcinoma through pathological examination, and the other one was confirmed as squamous cell carcinoma by biopsy.

Immunohistochemistry was used to study the expression of CD4, CD24, CD44, CK, and P63 in SMM of 10 cases (five cases of bronchus carcinoma, two cases of endometrial carcinoma, one case of stomach carcinoma, and two cases of hepatocellular carcinoma). Positive CD4, CD24, and CD44 were expressed in SMM tissue of seven cases (four cases of bronchus carcinoma, two cases of endometrial carcinoma, and one case of hepatocellular carcinoma), CK was expressed in six cases (two cases of bronchus carcinoma, two cases of endometrial carcinoma, one case of stomach carcinoma, and one case of hepatocellular carcinoma), and P63 was expressed in five cases (three cases of bronchus carcinoma, one case of endometrial carcinoma, and one case of stomach carcinoma).

## Discussion

The presentation of skeletal muscle metastases

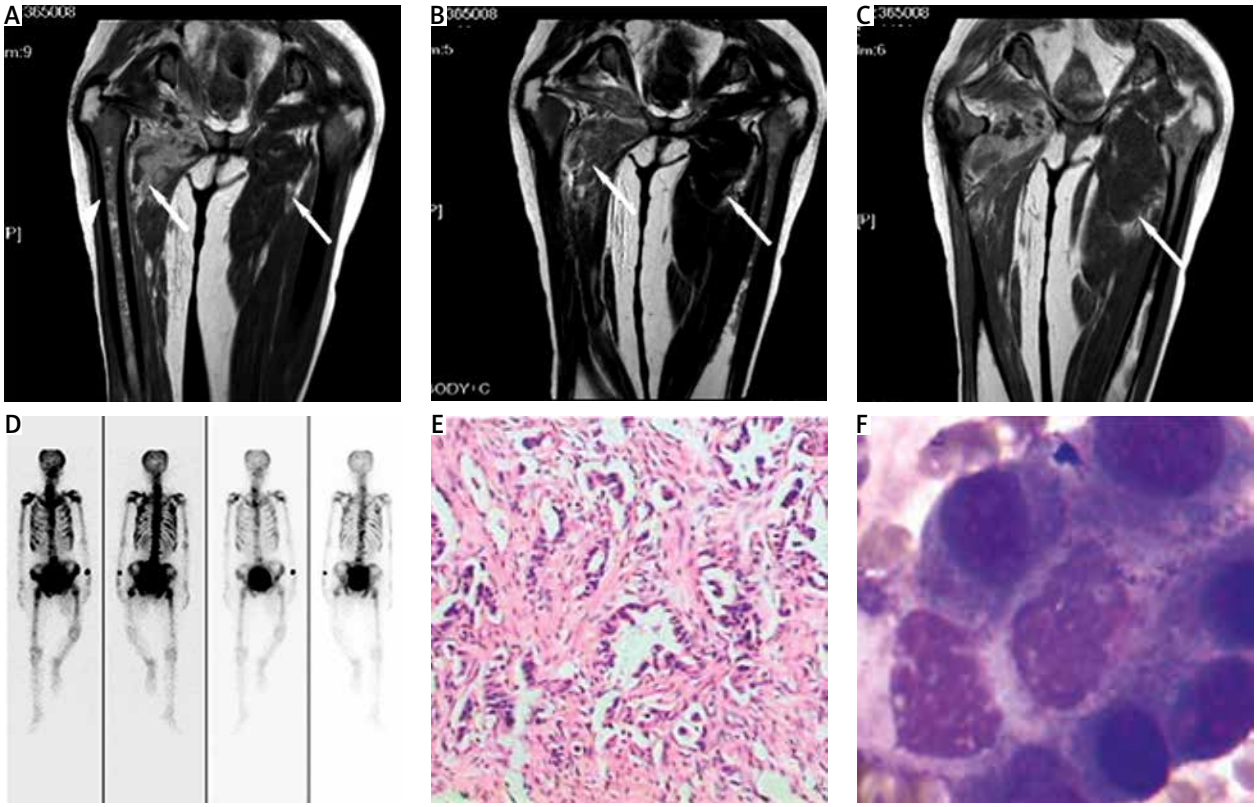


**Fig. 4.** Type III SMM complicated by bone destruction in a 53-year-old woman with a primary cancer of unknown origin. Persistent pain in the adductor longus had continued for 9 months, and motion of the hip joint was limited. MRI showed a soft tissue mass without clear boundaries, slightly hyperintense signal intensity (A, arrow) with mixed signal intensity in the bone marrow (A, arrowhead) in T1WI, and heterogeneous hyperintense signal intensity in T2WI (B, arrow). Enhanced MRI showed moderate enhancement (C, arrow). Radioactive uptake can be seen in the right femur (D). Soft tissue puncture confirmed adenocarcinoma muscle metastasis (E) (200× magnification). Bone marrow biopsy confirmed bone marrow metastasis (F)

Skeletal muscle is usually considered highly resistant to the mechanism of metastases from primary tumours [20–22]. However, metastases are not so rare in autopsy results [21–23]. There are some reports of epidemiological studies of muscle metastases, in which parameters such as age, location, and history were analysed. A report by Surov *et al*. [4] found that 13.7% of patients with muscle metastases presented with pain and soft-tissue swelling, and these patients had large lesions that were associated with massive muscle infiltration or destruction. In this study, 77.42% of patients complained of pain at the surface of the site, 41.93% of patients had localised swelling, and 32.26% of patients had both pain and swelling, which reflected a soft tissue bump with or without mass and required further examination to exclude skeletal metastases. Crundwell *et al*. [24] showed that SMM may develop following a trauma to the muscle; however, there was no history of muscle trauma in any of the cases in this study. Thus, any soft tissue mass should be investigated, whether or not it is accompanied by pain, with or without trauma. Surov *et al*. [4] showed that SMM was most frequently observed in the paravertebral, iliopsoas, and gluteal muscles. Our study found that SMM was most frequently observed in the iliopsoas muscle (26.3%), which was similar to the findings obtained by Surov *et al*. [4] and Koike *et al*. [17], followed by paravertebral muscles (21.1%) and upper extremity muscles (18.4%), but the appearance of lesions in the gluteus maximus was much less frequent (5.3%) in our study. The size of our samples (7.23 × 4.04 cm) was similar to that reported by Tuoheti *et al*. [15] (average diameter = 7 cm). Our results showed that the mean patient age was 57 years, which was similar to the results of Tuoheti *et al*. [15] and Surov *et al*. [4] Furthermore, the biopsy and pathology results showed that most lesions were derived from ade-

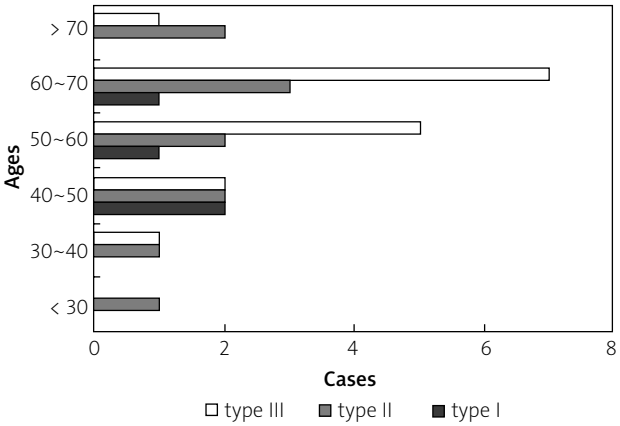


**Fig. 5.** The frequency of the different SMM subgroups according to patient age

nocarcinoma metastases or squamous cell carcinoma in our study. Immunohistochemistry was used to study the expression of CD4, CD24, CD44, CK, and P63 in SMM in 10 cases. CD4, CD24, CD44, and CK are expressed in many human malignant tumours [25–27]. P63 is a tumour suppressor gene P53 family member with enhanced expression in squamous cell carcinoma. It is a commonly used index abroad of squamous cell carcinoma of lung [28, 29]. In our study, P63 was expressed in all of the squamous cell carcinoma of lungs. It also could be concluded that patients over the age of 60 years frequently presented with a diffuse soft tissue mass or pain for no obvious reason, and with a lesion size of more than 7 cm. In this group, MRI should be used to exclude SMM.

### Magnetic resonance imaging characteristics of skeletal muscle metastases

In this study, most of the SMM cases showed heterogeneous iso-intensity in T1WI, heterogeneous hyperintensity in T2WI and TSE-SPAIR T2WI, and heterogeneous moderate enhancement. This finding is similar to the results of Koike *et al*. [17] and Lee *et al*. [9] and most cases showed the most remarkable hyperintensity in TSE-SPAIR T2WI, which suggests that TSE-SPAIR T2WI must be performed when SMM is suspected. Twenty-six patients underwent enhanced MRI examinations in our study, and they were found to have heterogeneous moderate enhancement, a finding which differed from the result of Koike *et al*. [17], in which patients showed significant enhancement and ring enhancement. The reason for this difference may be that eight of these 10 patients had Type II and Type III-2 lesions, and the lesions were relatively large, so heterogeneous moderate enhancement was detected. Fourteen cases showed feather-like changes, one of which showed feather-like enhancement. Munk *et al.* [10] reported feather-like changes in one case of their cohort, which suggested that the feather-like changes may be characteristic of SMM, but they should be distinguished from traumatic changes. Broome *et al.* [30] suggested that feather-like changes in the muscle are typical for partial muscle tears found post trauma. A putative mechanism for this finding is that the lesions show haemorrhage and oedema, and proliferation in gaps in the muscle bundle. However, the mechanism of feather-like changes associated with SMM in MRI has not been clearly elucidated and requires further study.

A study by Surov *et al.* [4] used CT techniques to study SMM and divided the CT radiographic findings into five different groups, which has provided a reliable basis for the diagnosis and the differential diagnosis of SMM. In our study, we combined analysis of MRI features of SMM and developed the '3-type 4-subtype system' for SMM, to develop a system which is beneficial for the diagnosis and the differential diagnosis of SMM. Four cases in the Type I subgroup involved the psoas muscle, had clear boundaries, and were not very large. This corresponded to the Type-1 and Type-2 patients in the CT study by Surov *et al.* [4]. Herring *et al*. [13] suggested that patients are able to receive benefit from radiotherapy or chemotherapy following surgical resection of SMM, but that only isolated SMM less than 4 cm in diameter should be considered for surgery, rather than biopsy [1, 31, 32]. In our study, the five-year survival for the four cases with focal-type Type I SMM post-surgical resection was 100%.

Of the Type II and Type III cases, in 14 cases, lesions showed feather-like changes, most of which were at the edge of the lesions. This observation needs to be distinguished from post-traumatic muscle tears and must also be distinguished from smooth muscle sarcoma and rhabdomyosarcoma. We further classified the Type III cases as being one of two subtypes based on clear or unclear boundaries. The Type III-1 cases showed a demarcated mass with clear limitation of the lesions and were less than 5 cm in diameter. The Type III-2 cases were characterised by a wider range of lesions with ill-defined boundaries and diameter less than 10 cm.

Our MRI findings differed from those of Surov *et al*. [4], whose major findings were obtained with CT. As is well documented, the soft-tissue resolution of MRI is superior to CT, so MRI is better able to show invasive features. As for the soft tissue changes, we believe that the feather-like changes may be a sign of diffuse invasion. Our results show that diffuse SMM with or without bone destruction is the most common type, and that focal lesions are not very frequent, which differs from Surov *et al*.'s [4] CT findings showing that focal lesions made up the majority of cases. Therefore, it is difficult to depict soft tissue invasion by CT alone, and the misdiagnosis rate was higher. Also, cancer epidemiology profiles differ between countries and regions. In Western, developed countries, breast cancer and intestinal cancer are common [1], while lung cancer and gastrointestinal cancer are less common. However, lung cancer, gastrointestinal tumours, and prostate cancer occur frequently in the urban population in China, which leads to different SMM manifestations between the two regions.

As a new technique of imaging, diffusion-weighted MRI (DWI), has been applied in clinical research recently. By exploiting and characterising diffusion of water molecules in muscle, DWI can provide information about tissue anatomy and the water molecules to evaluate skeletal muscle injury, inflammation, and metastases and determine the treatment [33–35]. DWI is increasingly considered as a helpful supplementary imaging tool for SMM, but no patients underwent DWI examination in this study.

### Differential diagnosis according to magnetic resonance imaging type of skeletal muscle metastases

The respective SMM subtypes must be differentiated from a number of other pathologies. (1) Single haematoma of skeletal muscle can present as feather-like changes, which is similar to SMM [36]. However, a history of definite trauma typically allows a differential diagnosis with Type I SMM [37]. (2) Haemangioma may appear with slightly higher signal intensity than muscle in T1WI. It may show a worm-like or punctuate hypointensity without feather-like changes in T2WI [38, 39]. (3) Synovial sarcoma occurs in the large joints and shows heterogeneous signal intensity with mainly an iso-intensity. The soft tissue infil-

tration from the tumour is irregular, and tumour thickness varies [40]. (4) Malignant fibrous histiocytoma is especially found in the deep parts of the legs. A bleeding lesion in the tumour appears with hyperintensity in T1WI, which could reflect high vascular invasion characteristics [41–43].

## Limitations

(1) The study was a retrospective study, thus there were selection bias and follow-up bias on patient selection, which could have affected the results. (2) This study included a small number of evaluated patients, which should be increased in the future. (3) DWI studies can provide additional information on soft tissue, which is now considered to be an effective method of assessment of soft tissue tumour cells; however, no patients underwent DWI examination in this study. We have already planned the next phase to include a prospective study of SMM with increased use of DWI.

In conclusion, skeletal muscle metastases are rare and may be easily misdiagnosed as primary soft tissue tumours or soft tissue trauma. MRI is currently widely used for the diagnosis of the tumour and differential diagnosis of other diseases. We found that an MRI presentation of heterogeneous iso-signal intensity in T1WI and heterogeneous hyperintense signal in T2WI with or without adjacent bone invasion with localised swelling and pain could be used to suspect SMM. SMM can be divided into three subtypes based on MRI features, such as the shape, tumour margins, and the presence of bone involvement, which is helpful for diagnosis and differential diagnosis of SMM.

*We would like to express our thanks to Engineer Yingsa Li (Philips Company) for providing technical assistance. We also express our thanks to International Science Editing for editing this article.*

*The authors declare no conflict of interest.*

**References**

1. Araki K, Kobayashi M, Ogata T, Takuma K. Colorectal carcinoma metastatic to skeletal muscle. Hepatogastroenterology 1994; 41: 405-8.
2. Menard O, Parache RM. Muscle metastases of cancers. Ann Med Interne (Paris) 1991; 142: 423-8.
3. Kozyreva ON, Mezentsev DA, King DR, Gomez-Fernandez CR, Ardalan B, Livingstone AS. Asymptomatic muscle metastases from esophageal adenocarcinoma. J Clin Oncol 2007; 25: 3780-3.
4. Surov A, Hainz M, Holzhausen HJ, Arnold D, Katzer M, Schmidt J, Spielmann RP, Behrmann C. Skeletal muscle metastases: primary tumours, prevalence, and radiological features. Eur Radiol 2010; 20: 649-58.
5. Schultz SR, Bree RL, Schwab RE, Raiss G. CT detection of skeletal muscle metastases. J Comput Assist Tomogr 1986; 10: 81-3.
6. Ouyang L, Jia QX, Xiao YH, Ke LS, He P. Magnetic resonance imaging: a valuable method for diagnosing chronic lumbago caused by lumbar muscle strain and monitoring healing process. Chin Med J (Engl) 2013; 126: 2465-71.
7. Jiang H, Wang ZC, Xian JF, Li J, Zhao PF. Age-related changes of normal adult inferior rectus muscle:analysis with dynamic contrast-enhanced magnetic resonance imaging. Chin Med J (Engl) 2011; 91: 1899-903.
8. Moon YL, Ahn KY, Moon SP, Lim SC, Venkat G. Subscapularis muscle metastases of duodenal adenocarcinoma: a case report. J Shoulder Elbow Surg 2010; 19: e18-21.
9. Lee BY, Choi JE, Park JM, Jee WH, Kim JY, Lee KH, et al. Various image findings of skeletal muscle metastases with clinical correlation. Skeletal Radiol 2008; 37: 923-8.
10. Munk PL, Gock S, Gee R, Connell DG, Quenville NF. Case report 708: Metastasis of renal cell carcinoma to skeletal muscle (right trapezius). Skeletal Radiol 1992; 21: 56-9.
11. LaBan MM, Tamler MS, Wang AM, Meerschaert JR. Electromyographic detection of paraspinal muscle metastasis. Correlation with magnetic resonance imaging. Spine (Phila Pa 1976) 1992; 17: 1144-7.
12. Glockner J, Sundaram M, White L. Incidence of solitary soft-tissue metastases revealed by MR imaging. AJR Am J Roentgenol 2002; 179: 1644.
13. Herring CL Jr, Harrelson JM, Scully SP. Metastatic carcinoma to skeletal muscle. A report of 15 patients. Clin Orthop Relat Res 1998; (335): 272-81.
14. Williams JB, Youngberg RA, Bui-Mansfield LT, Pitcher JD. MR imaging of skeletal muscle metastases. AJR Am J Roentgenol 1997; 168: 555-7.
15. Tuoheti Y, Okada K, Osanai T, Nishida J, Ehara S, Hashimoto M, Itoi E. Skeletal muscle metastases of carcinoma: a clinicopathological study of 12 cases. Jpn J Clin Oncol 2004; 34: 210-4.
16. Suto Y, Yamaguchi Y, Sugihara S. Skeletal muscle metastasis from lung carcinoma: MR findings. J Comput Assist Tomogr 1997; 21: 304-5.
17. Koike Y, Hatori M, Kokubun S. Skeletal muscle metastasis secondary to cancer – a report of seven cases. Ups J Med Sci 2005; 110: 75-83.
18. Schmidt GP, Reiser MF, Baur-Melnyk A. Whole-body imaging of the musculoskeletal system: the value of MR imaging. Skeletal Radiol 2007; 36: 1109-19.
19. Leslie H, Mary K, Christian Wittekind. TNM Classification of Malignant Tumours (7th ed.). Wiley-Blackwell, New York 2009.
20. Seely S. Possible reasons for the high resistance of muscle to cancer. Med Hypotheses 1980; 6: 133-7.
21. Acinas GO, Fernandez FA, Satue EG, Buelta L, Val-Bernal JF. Metastasis of malignant neoplasms to skeletal muscle. Rev Esp Oncol 1984; 31: 57-67.
22. Weiss L. Biomechanical destruction of cancer cells in skeletal muscle: a rate-regulator for hematogenous metastasis. Clin Exp Metastasis 1989; 7: 483-91.
23. PEARSON CM. Incidence and type of pathologic alterations observed in muscle in a routine autopsy survey. Neurology 1959; 9: 757-66.
24. Crundwell N, O'Donnell P, Saifuddin A. Non-neoplastic conditions presenting as soft-tissue tumours. Clin Radiol 2007; 62: 18-27.
25. Pruszak J, Ludwig W, Blak A, Alavian K, Isacson O. CD15, CD24, and CD29 define a surface biomarker code for neural lineage differentiation of stem cells. Stem Cells 2009; 27: 2928-40.
26. Asuthkar S, Stepanova V, Lebedeva T, et al. Multifunctional roles of urokinase plasminogen activator (uPA) in cancer stemness and chemoresistance of pancreatic cancer. Mol Biol Cell 2013; 24: 2620-32.
27. Han JB, Sang F, Chang JJ, et al. Arsenic trioxide inhibits viability of pancreatic cancer stem cells in culture and in a xenograft model via binding to SHH-Gli. Onco Targets Ther 2013; 6: 1129-38.
28. Parsa R, Yang A, McKeon F, Green H. Association of p63 with proliferative potential in normal and neoplastic human keratinocytes. J Invest Dermatol 1999; 113: 1099-05.
29. Terry J, Leung S, Laskin J, Leslie KO, Gown AM, Ionescu DN. Optimal immunohistochemical markers for distinguishing lung adenocarcinomas from squamous cell carcinomas in small tumor samples. Am J Surg Pathol 2010; 34: 1805-11.
30. Broome DR, Girguis MS, Baron PW, Cottrell AC, Kjellin I, Kirk GA. Gadodiamide-associated nephrogenic systemic fibrosis: why radiologists should be concerned. AJR Am J Roentgenol 2007; 188: 586-92.

31. Lampenfeld ME, Reiley MA, Fein MA, Zaloudek CJ. Metastasis to skeletal muscle from colorectal carcinoma. A case report. Clin Orthop Relat Res: 1990; 256: 193-6.
32. Lawrence W Jr, Donegan WL, Natarajan N, Mettlin C, Beart R, Winchester D. Adult soft tissue sarcomas. A pattern of care survey of the American College of Surgeons. Ann Surg 1987; 205: 349-59.
33. Noseworthy MD, Davis AD, Elzibak AH. Advanced MR imaging techniques for skeletal muscle evaluation. Semin Musculoskelet Radiol 2010; 14: 257-68.
34. Saupe N, White LM, Stainsby J, Tomlinson G, Sussman MS. Diffusion tensor imaging and fiber tractography of skeletal muscle: optimization of B value for imaging at 1.5 T. AJR Am J Roentgenol 2009; 192: W282-290.
35. Saotome T, Sekino M, Eto F, Ueno S. Evaluation of diffusional anisotropy and microscopic structure in skeletal muscles using magnetic resonance. Magn Reson Imaging 2006; 24: 19-25.
36. Nguyen B, Brandser E, Rubin DA. Pains, strains, and fasciculations: lower extremity muscle disorders. Magn Reson Imaging Clin N Am 2000; 8: 391-408.
37. Hasselman CT, Best TM, 4th HC, Martinez S, Garrett WE Jr. An explanation for various rectus femoris strain injuries using previously undescribed muscle architecture. Am J Sports Med 1995; 23: 493-9
38. Jenner G, Soderlund V, Bauer HF, Brosijo O. MR imaging of skeletal muscle hemangiomas. A report of 16 cases. Acta Radiol 1996; 37:140-4.
39. Lee TJ, Collins J. MR imaging evaluation of disorders of the chest wall. Magn Reson Imaging Clin N Am 2008; 16: 355-79.
40. Tang YM, Stuckey S, Lambie D, Strutton GM. Macroscopic vascular invasion in synovial sarcoma evident on MRI. Skeletal Radiol 2006; 35: 783-6.
41. Koplas MC, Lefkowitz RA, Bauer TW, Joyce MJ, Ilaslan H, Landa J, et al. Imaging findings, prevalence and outcome of de novo and secondary malignant fibrous histiocytoma of bone. Skeletal Radiol 2010; 39: 791-8.
42. Miller TT, Hermann G, Abdelwahab IF, Klein MJ, Kenan S, Lewis MM. MRI of malignant fibrous histiocytoma of soft tissue: analysis of 13 cases with pathologic correlation. Skeletal Radiol 1994; 23: 271-5.
43. Park SW, Kim HJ, Lee JH, Ko YH. Malignant fibrous histiocytoma of the head and neck: CT and MR imaging findings. AJNR Am J Neuroradiol 2009; 30: 71-6.

**Address for correspondence**

**Shinong Pan**
No. 36, Sanhao Street, Heping District
110004 Shenyang, China
e-mail: 1982liqi@163.com

**Submitted:** 8.06.2014
**Accepted:** 19.11.2014